SPE 38699

Applications and Derivation of a New Cased-hole Density Porosity in Shaly Sands

R.C. Odom, SPE, Computalog Research, Inc.; G.P. Hogan II, SPE, Computalog Wireline Services; B.W. Crosby, SPE, Computalog Wireline Services; M.P. Archer, Chevron U.S.A., Inc.

This paper was prepared for presentation at the 1997 SPE Annual Technical Conference and Exhibition held in San Antonio, Texas, 5 _ 8 October 1997.

Abstract

Recently, the physical foundations and derivation of a cased-hole, density-based porosity have been developed for the Computalog PND-S pulsed neutron system. The utility of this measurement is demonstrated in applications to reservoir analysis problems in sand-shale sequences of the Gulf Coast and offshore Gulf of Mexico. This cased-hole density porosity is based on the attenuation of gamma rays produced by inelastic scattering of fast neutrons. These fast-neutron reactions create a dispersed gamma-ray source in close proximity to the accelerator, and the subsequent transport of these gamma rays is strongly affected by the density of the formation. The higher energies and larger geometric scales of this technique give it sufficient penetration to measure a cased-hole density porosity that compares favorably to the open-hole, gamma-gamma density.

Applications (in combination with the cased-hole neutron porosity) include providing porosities where hole conditions make open-hole logging unviable, and in old wells where no modern porosity logs exist or the data is of questionable quality. This measurement can be utilized in cased-hole prospecting by differentiating low porosity from gas-filled porosity. Reservoir monitoring applications include: hydrocarbon typing, estimating pressure changes in gas reservoirs, and monitoring fluid level and hydrocarbon type changes.

Following discussions of the derivation and possible applications, several log examples from the Gulf Coast and offshore Gulf of Mexico demonstrate the uses of the system and the correlation with the conventional open-hole density porosity.

Introduction

The density-neutron crossplot porosity has long been the workhorse of the log analyst. The strength of this union lies in the fact that these two porosities have roughly equal and opposite errors with respect to shale content and gas content. When these measurements are used together, a more accurate estimate of the porosity is obtained. The overlay of these porosities on the well log can be used to visually estimate the shale and fluid content of the logged formations.

Traditionally, in cased-reservoir analyses, the main source of porosity is the hydrogen-based neutron porosity. The neutron radiation is capable of penetrating the well casing and cement and affecting measurable reactions in the formation. The

spatial distribution of thermal neutrons (near-to-far ratio) is related to the hydrogen content of the formation. Given the assumptions that the rock matrix does not contain hydrogen and the pore fluid is water, the hydrogen content is mapped into a porosity measure. Of course, these assumptions create errors in formations with shale in the matrix and/or gas in the pore fluid.

In order to have sensitivity to gas-filled porosity versus low porosity (gas vs. tight), current versions of the competitive pulsed neutron systems in the Gulf Coast market have incorporated detector counting bins during the source pulse to measure gamma rays created by inelastic scattering. The count rate during the source pulse is placed in simple ratio algorithms, and qualitative empirical relations are developed.[1]

In previous publications[2,3,4], it has been demonstrated that the formation density can be isolated and measured using gamma rays created from inelastic scattering of fast neutrons. This paper describes the continuous process of making this a more accurate and quantitative measurement. In the following section, we will briefly describe the unfolding processes required to measure the effects of the formation density on the received inelastic signal. Currently, the extracted density parameter undergoes a scalar mapping to normalize the well-bore effects. The normalization is facilitated by calibration checks to core data, offset wells or local sections with open-hole data. The end result is a density porosity (PN density) similar to the open-hole, gamma-gamma density porosity (OH density). In the Characterization of Measurements section that follows is a discussion of the development of a prototypical borehole compensated (BHC) algorithm. In this BHC algorithm the measurements of borehole parameters are enfolded, so that external calibration data is not required. To promote the readability of this paper, we shall try to be brief and concise in the measurement theory section. The real points of interest are the applications in the log examples. The capability to measure the density behind casing is a powerful reservoir analysis tool. In the several log examples, the reader should gain some appreciation of the utility of this measurement in reservoir analysis and the correlation to the open-hole, gamma-gamma density.

Hardware Description

The measurements, applications and log examples discussed herein are based on data acquired with the standard PND-S system.[2] The through-tubing capable sonde (1.625 inch or 1.6875 inch diameters) produces pulses of 14 MeV neutrons and collects gamma-ray data from a 1 inch by 4 inch near NaI detector and a 1 inch by 6 inch far NaI detector. The incident gamma rays are segregated into time- and energy-dependent counting bins.

The pulse frequency and pulse width are adjusted to optimize the specific measurement sequence from the surface logging system. The firing cycle is a selected mix of a Servo Mode, with a frequency servoed to match the formation sigma in the range 200 Hz to 1000 Hz, and an Inelastic Mode, with a fixed frequency of 1428 Hz. Data from the Servo Mode are used to measure the formation sigma and neutron porosity; data from the Inelastic Mode are used to measure the PN density porosity, borehole parameters, and saturation from inelastic scattering spectroscopy (Carbon/Oxygen logging). The structure of the counting bins for the Inelastic Mode are diagramed in Figure 1; the spectroscopy bins are shown but are not used in the density-porosity measurement.

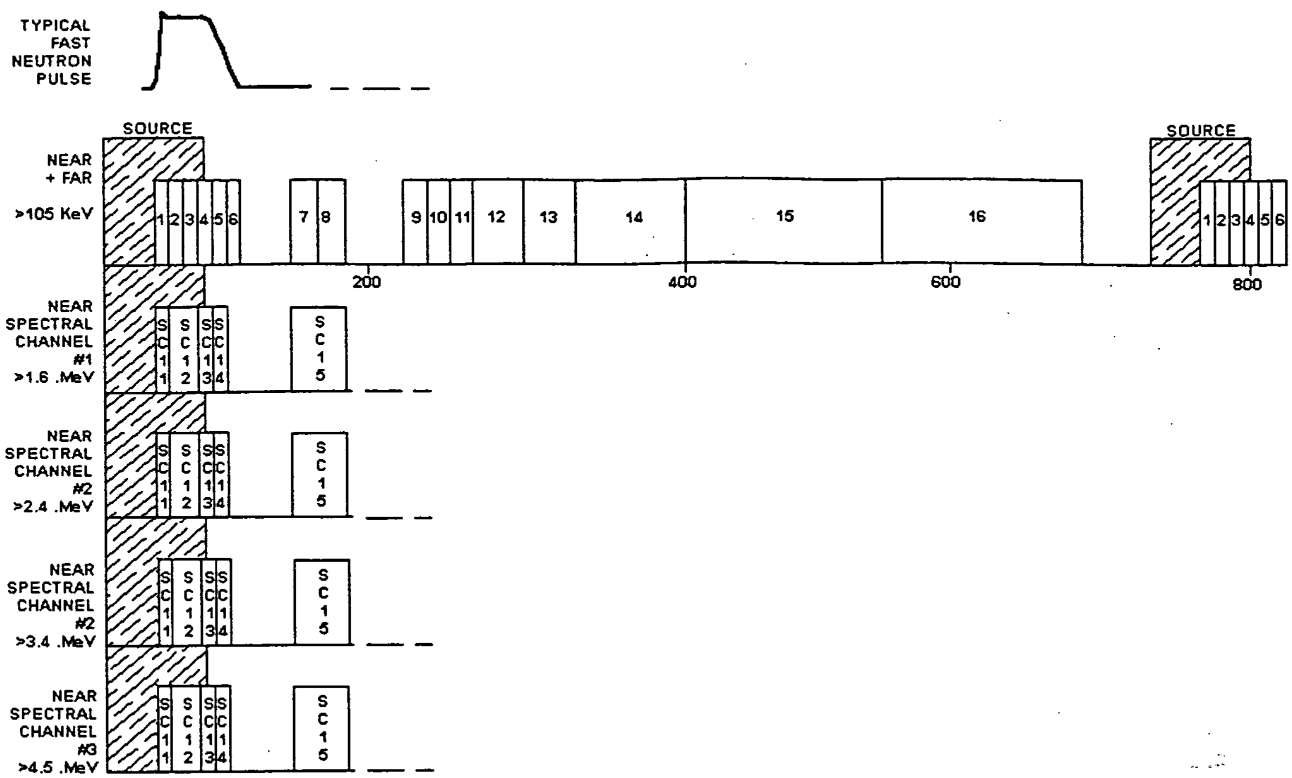

Figure 1 - A typical fast-neutron pulse and bin-timing diagram for the Inelastic Mode of the PND-S system (Version 9.3 and 9.4 specification).

Measurement Concepts

During the pulse of the fast neutrons, inelastic scattering with incident nuclei create a dispersed gamma-ray source centered around the accelerator (refer to Figure 2). In the fluid-filled, cased-borehole environment, the fast neutrons required to generate these high-energy threshold reactions have very short lives and paths. This means that the gamma-ray source will be in close proximity to the accelerator, and the instantaneous shape is similar to the source pulse. Once created, the gamma rays spread throughout the geometry, and the transport is attenuated by scattering collisions with electrons. Thus, there is an electron-density component as the gamma-ray signal is transported to the detectors.

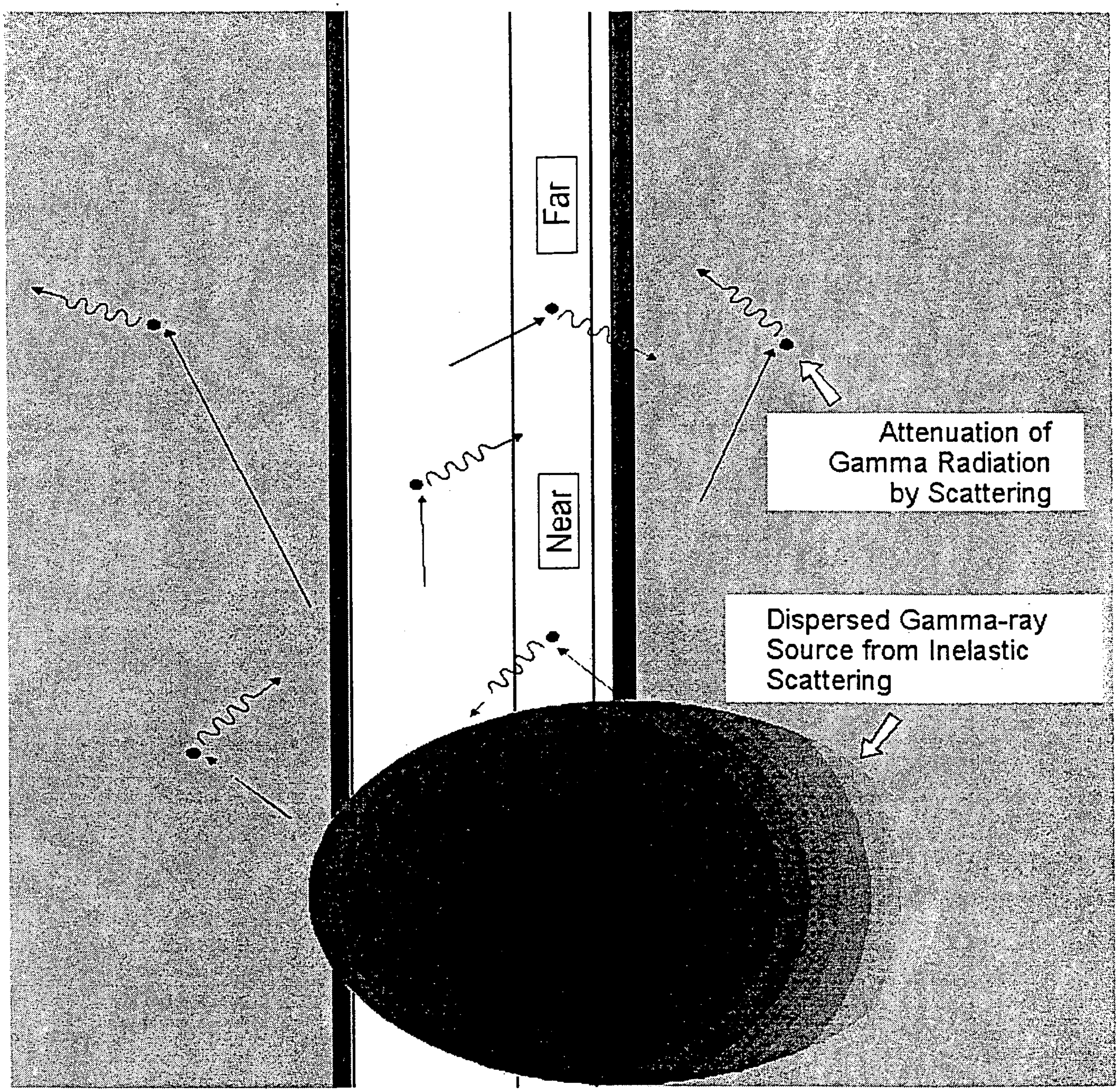

Figure 2 - Conceptual diagram of the PND density measurement physics. A gamma source is created from inelastic scattering of fast neutrons, and the subsequent transport of the gamma rays is attenuated by the density of the media.

Discussions of the assumptions required to convert the electron density to the bulk density can be found in the paper by Tittman and Wahl.[5] In that paper, the authors also describe the necessity that Compton scattering is the dominant mechanism for attenuation of gamma rays to minimize the effects of chemical composition of the media. The gamma-ray source energy should be in the range 0.1 MeV to 2.5 MeV to assure that Compton scattering is the dominant reaction type.

The near and far detectors have a lower-level discrimination at 0.105 MeV; this satisfies the lower energy bound.Figure 3 shows a typical gamma-ray spectra of the near detector in a water tank, and we note that the high-energy gamma rays (capable of pair-production interactions) are only a small percentage of the total gamma-ray signal. Although the inelastic reactions produce higher-energy gamma rays, the attenuation is predominately Compton scattering.

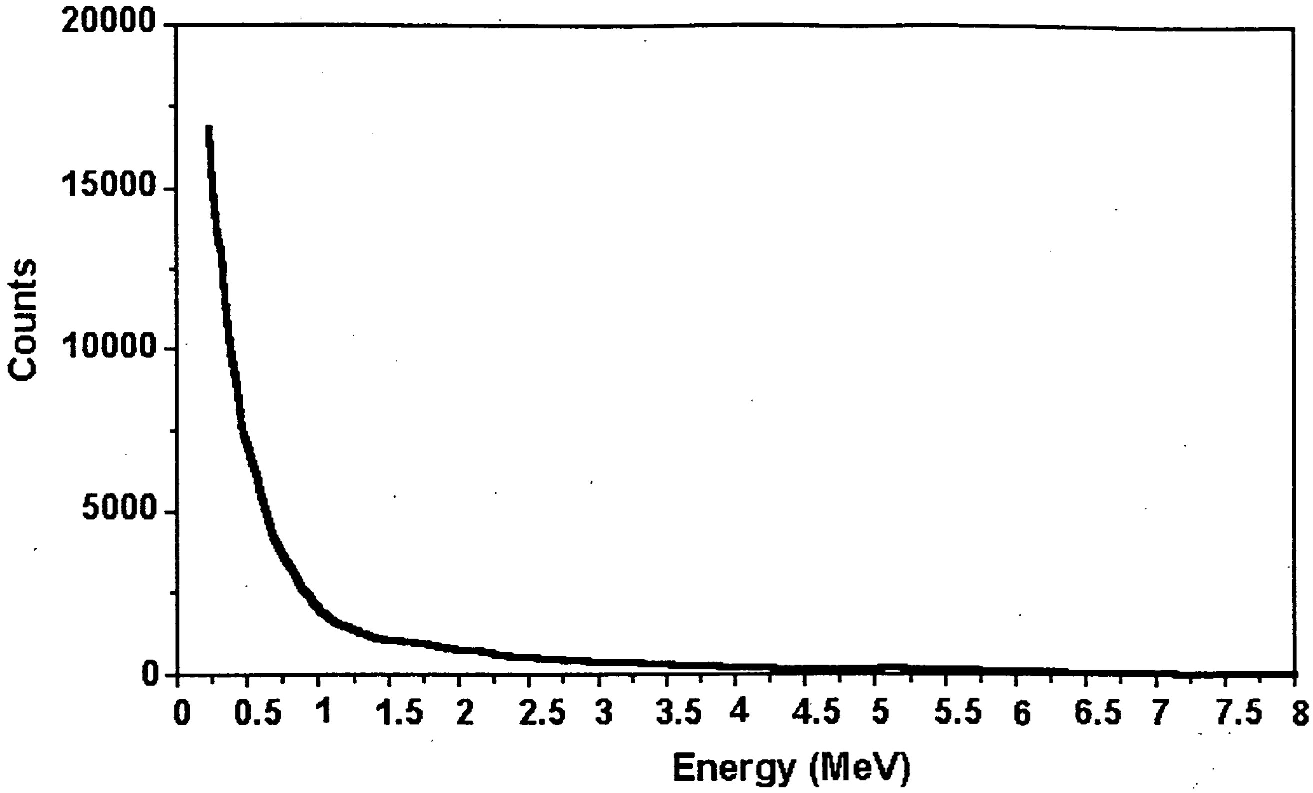

Figure 3 - Typical gamma spectrum during the source pulse for the near detector in the water tank.

It was intended that the attenuation of the inelastic gamma rays could be exploited to resolve the "gas vs. tight" ambiguity of the neutron porosity. Unfortunately, the deconvolution of the density component is not a simple matter. As shown inFigure 4, the gamma rays measured by detectors during the source pulse are a mix of several different reactions and are influenced by several dissimilar parameters. Unless the response parameters can be separated, measurements during the source pulse are inherently under-determined; in analogy, it is trying to count apples given the total pieces of fruit.

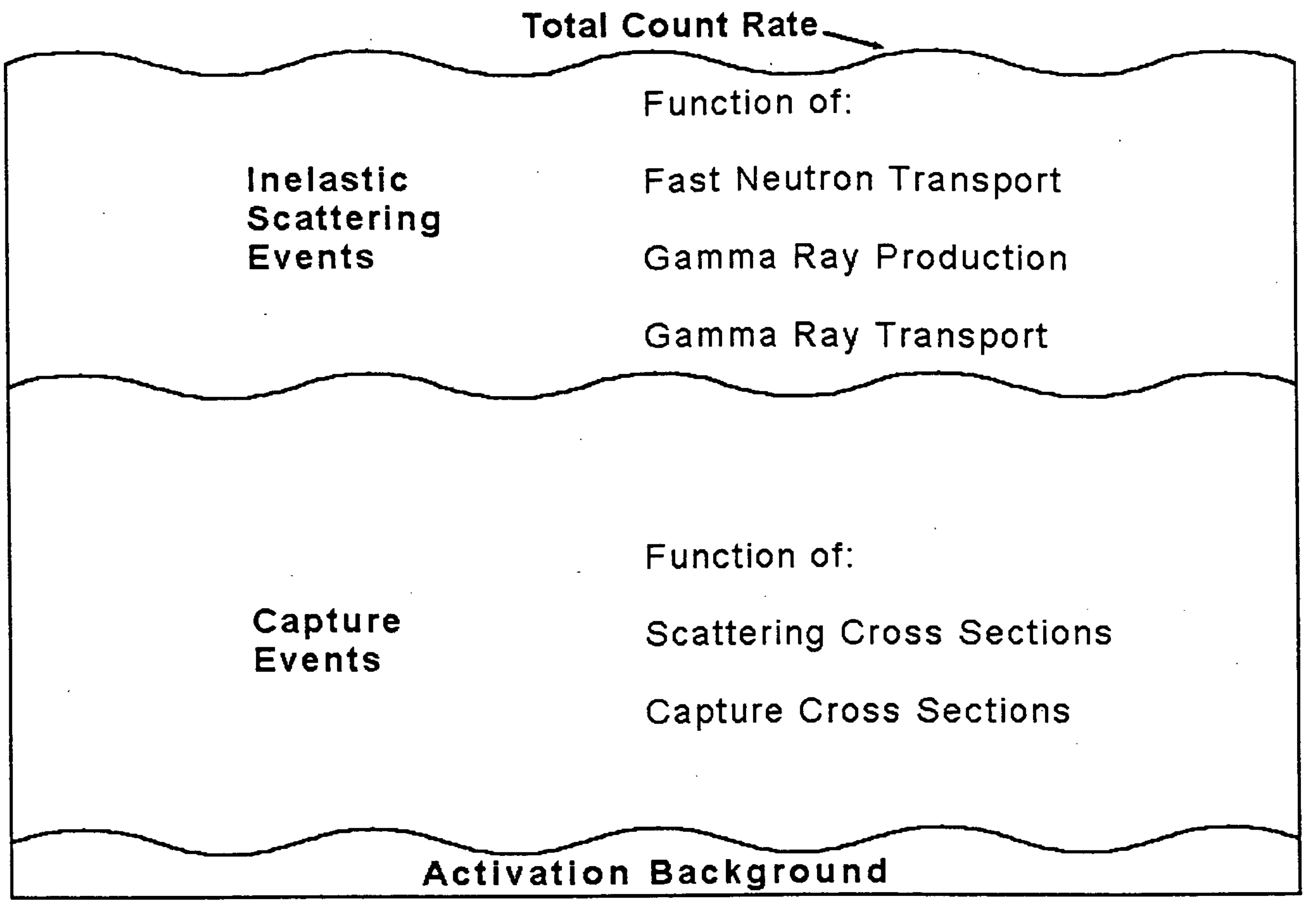

Figure 4 - Conceptual diagram of the counts measured during the source pulse.

Gamma rays received during the source pulse are a varying mix from three main reaction types: neutron activation, thermal neutron capture, and inelastic scattering. The activation background is generally less than one percent and is easily measured and removed. The count rate of capture reactions during the source pulse are a function of the scattering cross sections (the amount of hydrogen and steel) and the capture cross sections (the formation and borehole sigmas). The received inelastic signal is a function of three parameters.

1. Fast-neutron Transport is a function of the high-energy scattering cross sections. The spatial distribution of the fast neutrons determine the spatial distribution of the gamma-ray source.
2. Gamma Production is a function of the density and chemical composition (more specifically the isotopic composition) of the media. The number and type of reaction targets determine the number of gammas created.
3. Gamma Transport is a function of the electron density and determines the attenuation of gamma rays (this is the density parameter to be measured).

The first step in the deconvolution of the detector signal during the source pulse is the removal of the counts related to the capture signal.[6] The importance of this step is demonstrated in Figure 5. This is a typical sample for the far detector in an oil sand with 5-½ inch casing and a saltwater-filled borehole. The far detector bins are represented as points, and

hypothetical shapes of the capture and inelastic signals are diagramed. In analyzing the figure, we note that the capture signal is responsible for almost half of the counts received during the source pulse for this specific environment. After removing the counts from capture reactions, the total inelastic count rate at a detector can be mapped into the formation density given: the source-to-detector spacings are large enough to make the Gamma Transport the dominant parameter in the received signal, and there are minimal variations in the gamma-source distribution and strength. The resolved inelastic count rate is mapped to density via a logarithmic transformation. This semi-quantitative measurement is then normalized using a scalar mapping to remove the effects specific to the well-bore environment. The logarithmic mapping of the total count rate into density is the basis of the IPHI/FPHI porosities[4] used in Log Examples # 1 and # 2.

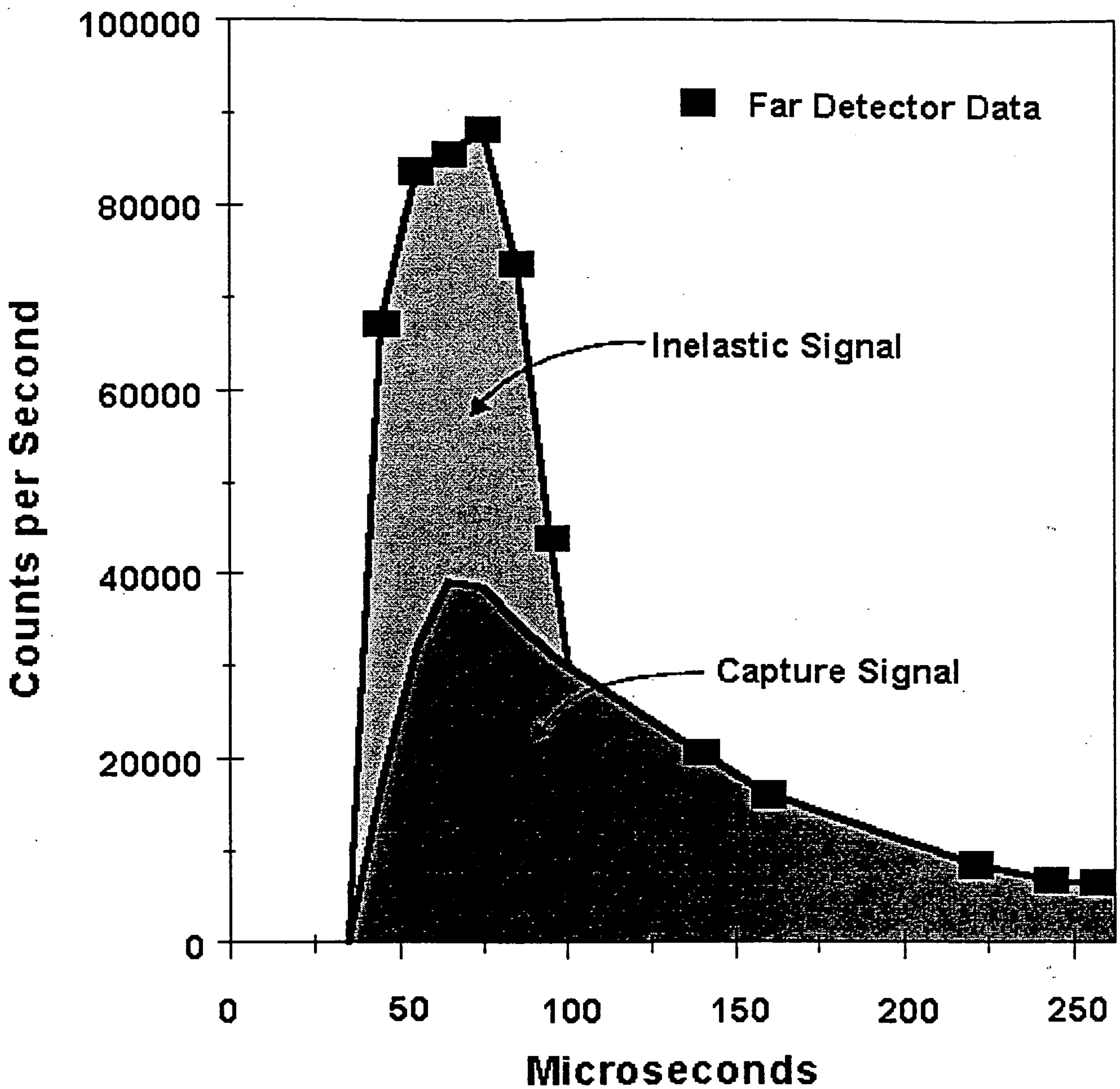

Figure 5 - Typical bin data for the far detector in an oil sand and the shapes of the capture and inelastic signals.

In the high-porosity environments typical of the Gulf Coast and offshore Gulf of Mexico, the abundance of hydrogen assures that the gamma source is contracted, which maximizes the spacing. Even though the effects on the total inelastic rate of variations in the gamma-source distribution are minimized at large spacings, they are still present as noise or undesirable responses. Further, to illustrate the dependence on the size and strength of the gamma source, consider the tight vs. gas problem. In both situations the hydrogen density has dropped, making the size of the gamma-ray source larger, and in the tight case the increased density means there are more inelastic targets (such as oxygen nuclei) to hit. The net result is that the total count rate may go up in both cases (compared to a porous water sand), and we are back to an ambiguous response. A similar situation is diagramed in Figure 6. In this figure the inelastic count rates, as a function of spacing, are shown for a tank of water and a 2.2 p.u. limestone block with an 8 inch freshwater-filled borehole. In the low-porosity limestone block, the fast neutrons travel farther and hit more oxygen nuclei, and we note that the gamma source variation has completely masked the density parameter. The near rate went up for the high-density block, and the far showed no density sensitivity.

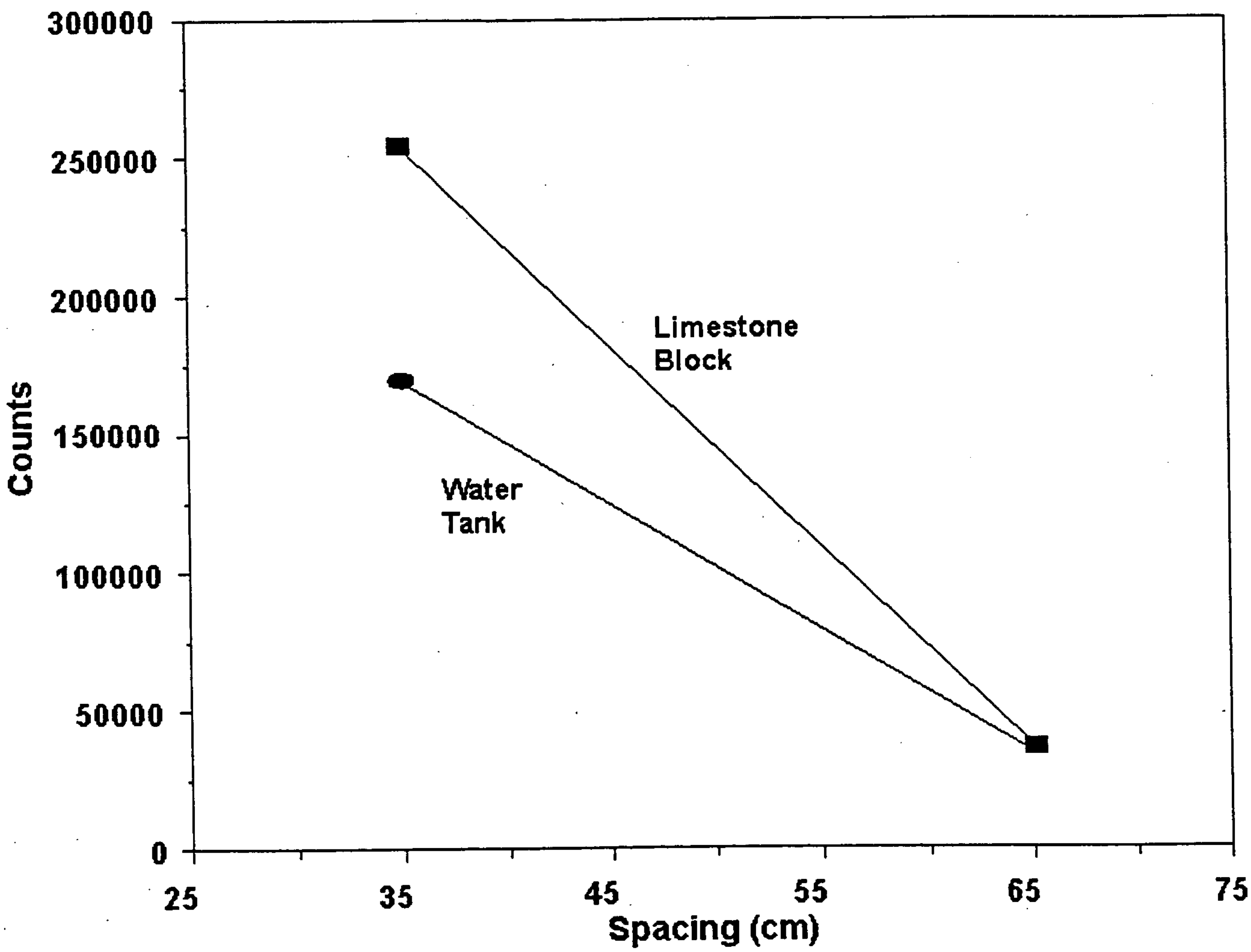

Figure 6 - Data from a water tank and a 2.2 p.u. limestone block (8 inch freshwater borehole).

Figure 6 - Data from a water tank and a 2.2 p.u. limestone block (8 inch freshwater borehole).

Invariance to gamma-source size and strength are developed using a more exact model for density measurement based on the differential signal from two detectors. The measurement LRHO, the gamma-ray diffusion length, is derived from a model of Boltzmann's Equation.[5] The differential measurement uses the inelastic signal at the near as the source and measures the subsequent attenuation of gamma transport to the far. Looking again at the ambiguity posed in Figure 6, given the centric geometry, LRHO can be viewed as a spatial die-away parameter which describes how the gamma radiation drops as a function of spacing. We note that for the limestone block the drop in the radiation has a steeper slope, which relates to higher attenuation (higher density) between the two detectors. Even though the two points have strongly different gamma-source distributions, the LRHO model accurately describes the density at these two porosity end-points. Through analysis of the theoretical model and empirical data, gamma-source invariance can be shown over the entire porosity range. Being a differential measurement implies there are differences of random variables (the detector count rates); thus, the statistical precision is less than with the IPHI/FPHI porosities. However, invariance to the uncertainties inherent in the total count rate more than make up for the diminished precision.

A more exact model will allow for a more straightforward quantification of the PN density response. As described, LRHO is inversely proportional to the density. The measured LRHO is an apparent measurement; it is the sum of transport in the formation and "leakage" transport in the borehole. As with the IPHI/FPHI porosities, this leakage term is assumed constant, and the LRHO response is normalized for the environment.

Characterization of Measurements

The many geometries, hardware, borehole fluids, etc. commonly encountered in cased reservoir analysis yield a massive characterization task. Characterization for a finite number of parameters may condemn certain environments (out of the norm) to semi-quantitative results. Currently, most of the characterization of these measurements has been in comparison to open-hole porosities. Fortunately, since these measurements are part of the standard PND-S acquisition system, a synergy can be exploited. The data that is required for the PN density porosity is part of the standard data set; this allows the testing of hypotheses and characterization techniques on all routine PND-S analyses. A tremendous amount of real field data has been studied to develop characterization algorithms for this measurement.

The OH density tool is a pad device, and the characterization of the measurements is based on good contact between the formation and the pad. The geometry of the PN density is centric rather than focused from the pad face; thus, the borehole becomes an intrinsic part of the measurement. The PND-S system has many available measurements of formation and borehole parameters. To test if these ancillary parameters can be used to drive a stand-alone BHC algorithm, a prototype multi-parameter algorithm was designed.

The characterization data from a set of 12 (sandstone) wells were used to develop a multi-parameter polynomial mapping of the PND-S measurements into the neutron (AIPN) and the density (AIPD) porosities. The characterizations covered approximately 15,000 half-foot samples from wells in various locations across the Gulf Coast and offshore. The wells were mostly 7 inch casings in 9 to 10 inch boreholes; three wells were 5-½ inch casing, and 5 wells were logged in 2-7/8 inch tubing inside 7 inch casing. If the BHC algorithm can get a good fit in these many different environments, this would suggest that the information embedded in the PND measurements is sufficient to automatically normalize the PN density porosity.

The fit of the prototype algorithm is diagramed in Figure 7. Given the uncertainties in both the PN density and the OH density, the mean-squared error of 2.77 p.u. is consistent with the accuracy of the case-specific characterization. A similar study of 11 wells in the low-porosity, mixed-litholology environments, common to the Permian Basin, demonstrated similar results with a mean-squared error of 3.24 p.u. across the 17,500 half-foot samples. The polynomial mapping (using one set of coefficients for the sandstone wells and another set for the carbonate wells) was able to automatically normalize across both of these large sets of conditions to make quantitative density measurements. The well in Log Example # 4 was part of the set of 12 (sandstone) wells, and the prototypical algorithm outputs are plotted with the open-hole porosities.

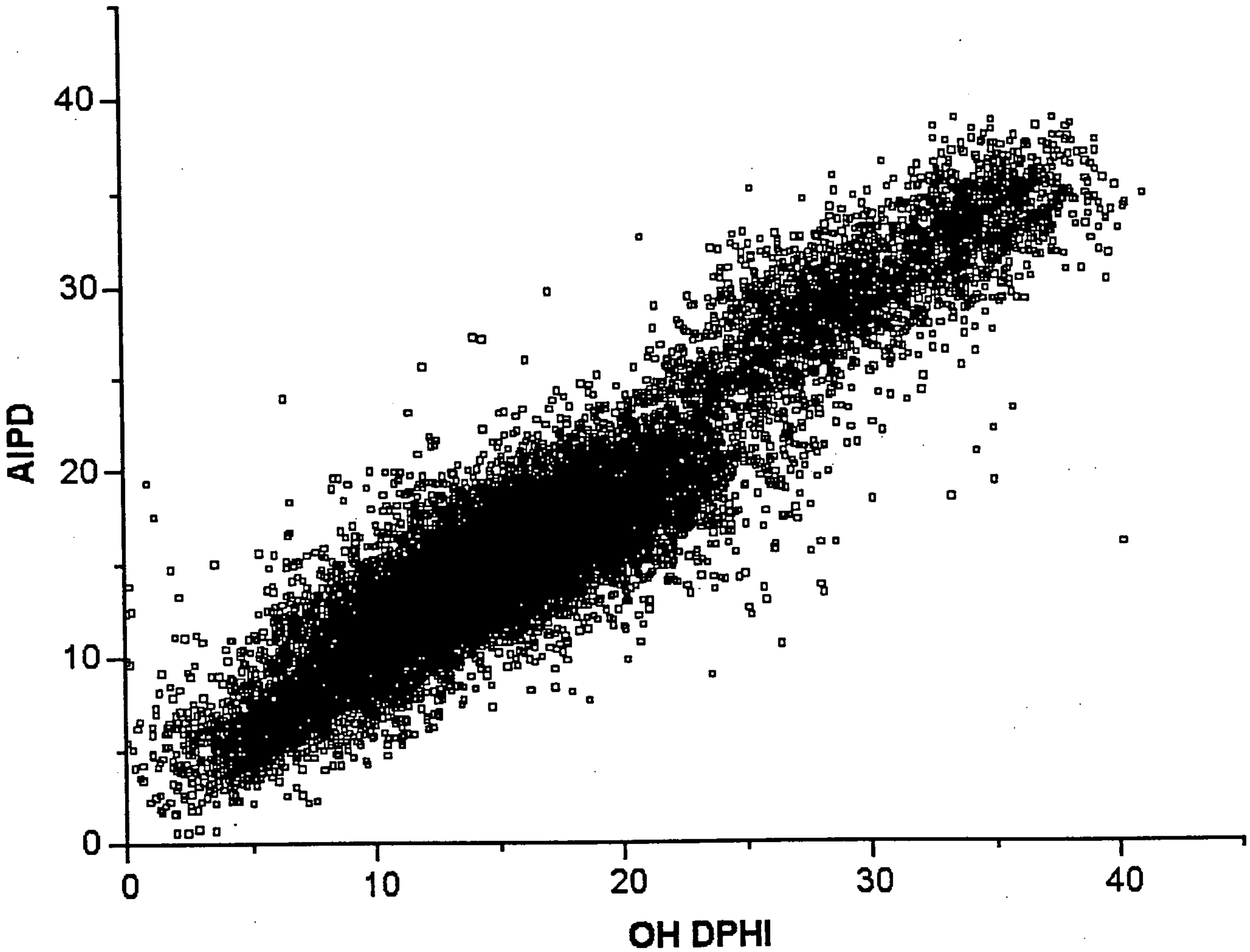

Figure 7 - Crossplot of the density porosity output from the prototypical BHC algorithm versus OH density porosity for the 12-well (sandstone) characterization study.

Considerations in Applying this Technology

To optimize results when applying the cased-hole density measurements to a specific well, the borehole geometry should be consistent, and the casing should be well cemented. The borehole should be filled with water (or oil). In gas-filled boreholes the lack of shielding reduces the relative amplitude of the formation signal, and several passes may be required to attain an acceptable level of precision. Similar to the gas-filled borehole, larger casing sizes will have lower "signal/leakage" ratios.

To improve the accuracy, some local information is required to normalize the specific borehole effects. Core data, open-hole logs in other sections of the well, or offset wells are often used. If these are not available, some general field knowledge and the thermal neutron ratio porosity RPHI can be used to improve the semi-quantitative density parameters

This density porosity comes from the inelastic burst firing which is only part of the firing cycle. Generally, to get quality

pulsed neutron capture data and the density porosity, the logging speed is slowed to 6 to 12 feet per minute.

Applications

This technology can be applied to many problems in reservoir analysis and monitoring. Some of the successful applications include:

Replacement of open-hole porosities in wells where open-hole data could not be obtained.

Replacement of, or in combination with, the open-hole density where hole rugosity or invasion makes the open-hole density questionable.

Monitoring hydrocarbon type changes and movements within the reservoir.

Pressure monitoring of gas reservoirs.

Small-diameter boreholes such as deepenings and sidetracks.

Cased-hole prospecting in old wells with limited porosity data.

Log Example # 1 (Refer to Figure 8).

The first application comes from a workover project on an offshore Gulf of Mexico well. The original 1986 open-hole porosity overlay is used as a base log; the 1996 PND-S porosity overlay is applied to diagnose current reservoir conditions. The well has a 8-½ inch bit size and is cased with 7 inch casing. The PND-S was logged through a gravel pack assembly (which is far less than ideal conditions), and the borehole effects on cased-hole porosities are normalized to the base open-hole porosities.

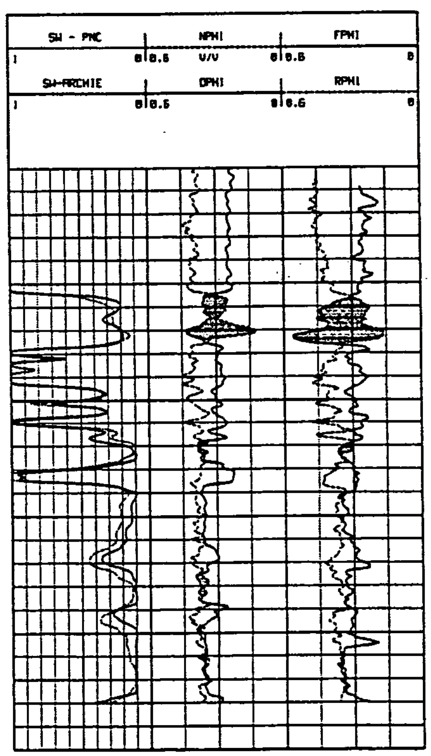

Figure 8 - Log Example 1 is an application in reservoir monitoring. The base OH porosities and saturation are from 1986; the PND porosities and saturations describe current (1996) reservoir parameters.

The technology was applied to two main analysis problems: 1) Has there been movement of the gas-oil contact and an associated pressure decrease relating to cross-fault communication with another reservoir block? 2) In planning the recompletion, information is needed to target the oil production and estimate current reservoir pressure.

In comparing the porosity overlays of Figure 8, it can be noted that the gas-oil contact has not moved, but the current gas-effect cross-over in the gas lobe has increased indicating the gas pressure has decreased. In addition, the current water saturations are calculated and are consistent with virgin saturations. Uncertainties in the correlation suggested to error on the safe side, and the completion was set up for 2,400 p.s.i., the virgin reservoir pressure. The well was completed in the oil section, and the reservoir pressure was found to be 1,400 p.s.i. Due to the fact that the gas lobe was known to have pressure communication with the oil section of the sand, the reduced pressure of 1,400 p.s.i. confirmed the cross-fault communication scenario.

Log Example # 2 (Refer to Figure 9).

This well is from offshore in the Gulf of Mexico and demonstrates using MWD and cased-hole logging as an alternative to open-hole logging. This is a new well drilled in 1996; the bit size is 6-¾ inch, and the PND-S log was run after setting 5-½ inch casing. The MWD resistivity/gamma-ray, logged while drilling, is useful in delineating the sand sequences and water saturations in the reservoir. The primary purpose of the PND-S is to determine hydrocarbon types in the sand members so the completion can be planned to target the desired production. In an offset well the sand member marked "Sand B" contained gas. In this down-dip well, the target was oil production from "Sand B". Analysis of the PND-S data affirmed that this member was oil, and the well was completed over this interval with production of 680 BOPD and 131 MCFD. The porosities in this sequence are fairly consistent (tight porosity is not a concern); the cased-hole crossplot technique allows the generation of realistic porosities with light hydrocarbons in the pore space.

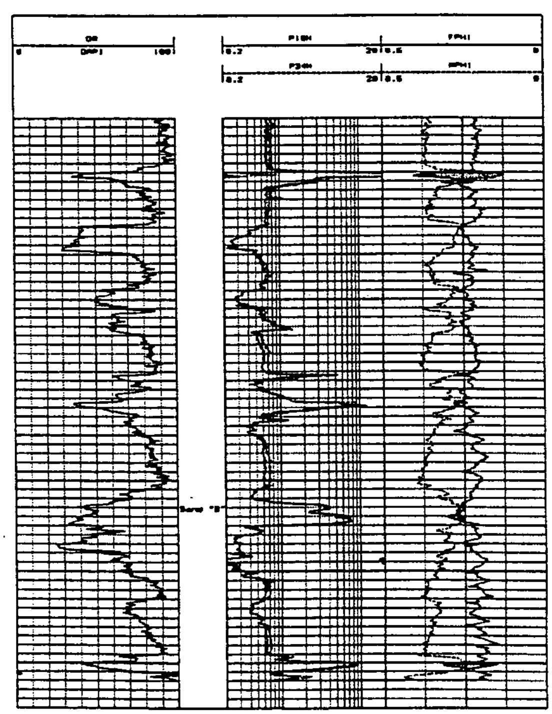

Figure 9 - In Log Example 2, MWD resistivity and cased-hole porosities are used for reservoir description on a new completion.

Log Example # 3 (Refer to Figures 10, 11 and 12).

This example uses the correlation of the open-hole crossplot to the cased-hole crossplot for quality control of the log database. The well is offshore in the Gulf of Mexico; it was drilled in 1990 with a 6-¾ inch bit size, and 5-½ inch casing was set. The workover target was oil production in the sand shown in Figure 12. From data in offset wells, the top of this sand is thought to be gas.

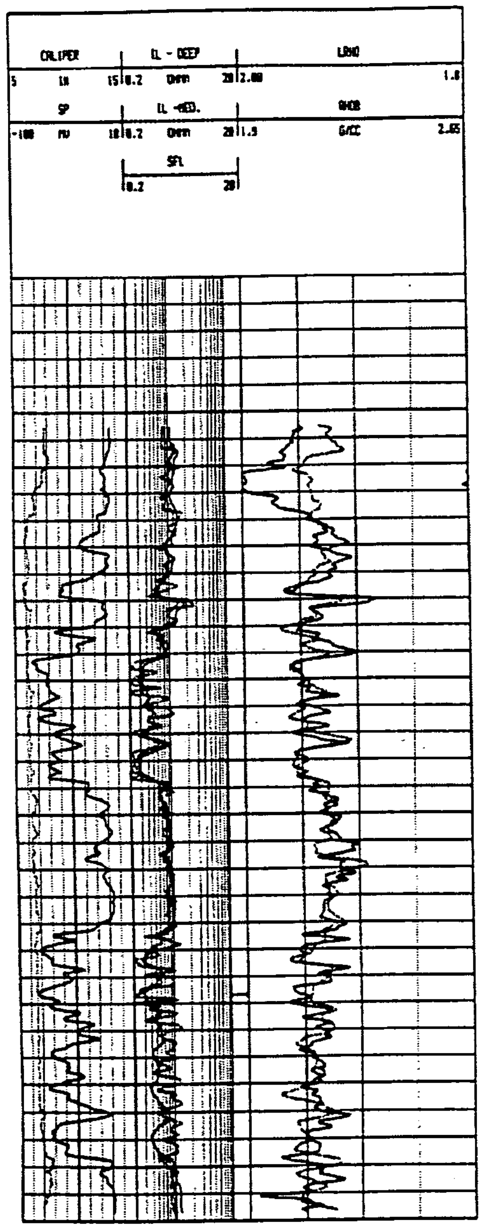

Figure 10 - Log Example 3 uses the cased-hole density to replace a questionable OH density run in 1990. In sections, like this water-sand sequence, the OH density seems to be correct, and the LRHO density parameter is normalized for the borehole environment.

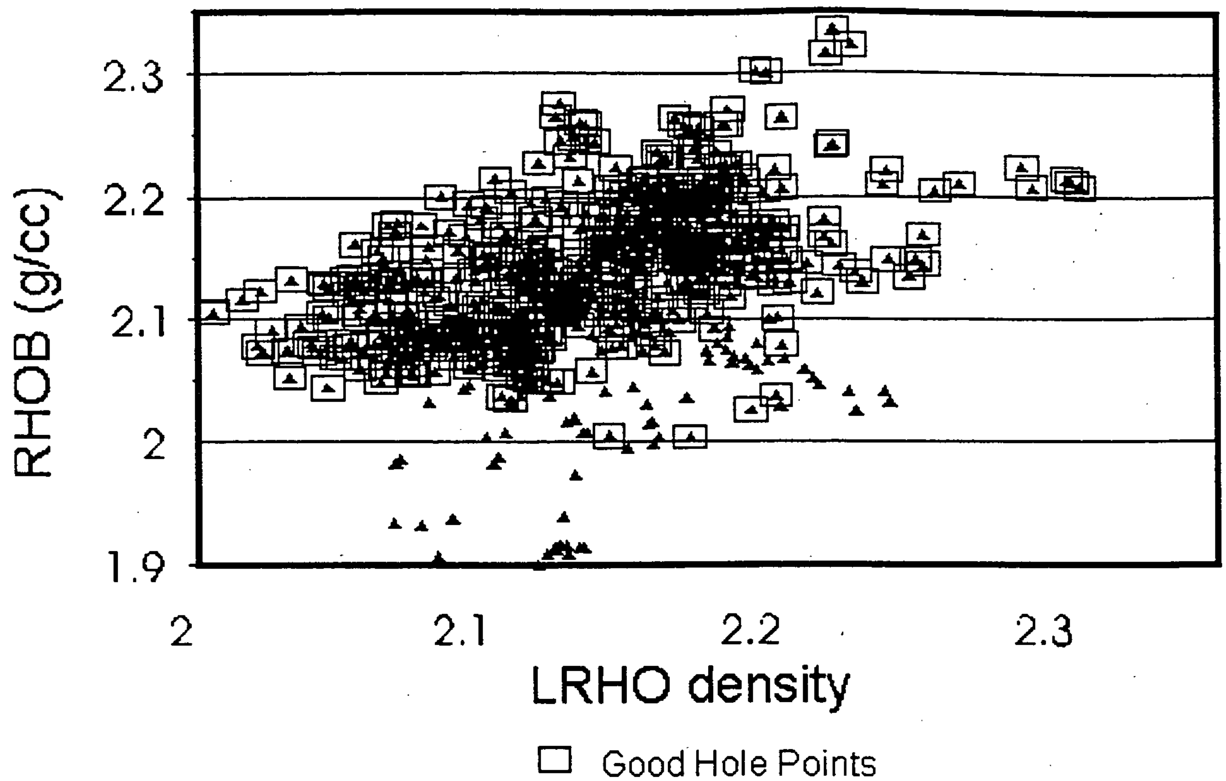

Figure 11 - Crossplot of the normalization fit over the water-sand sequence in Figure 10.

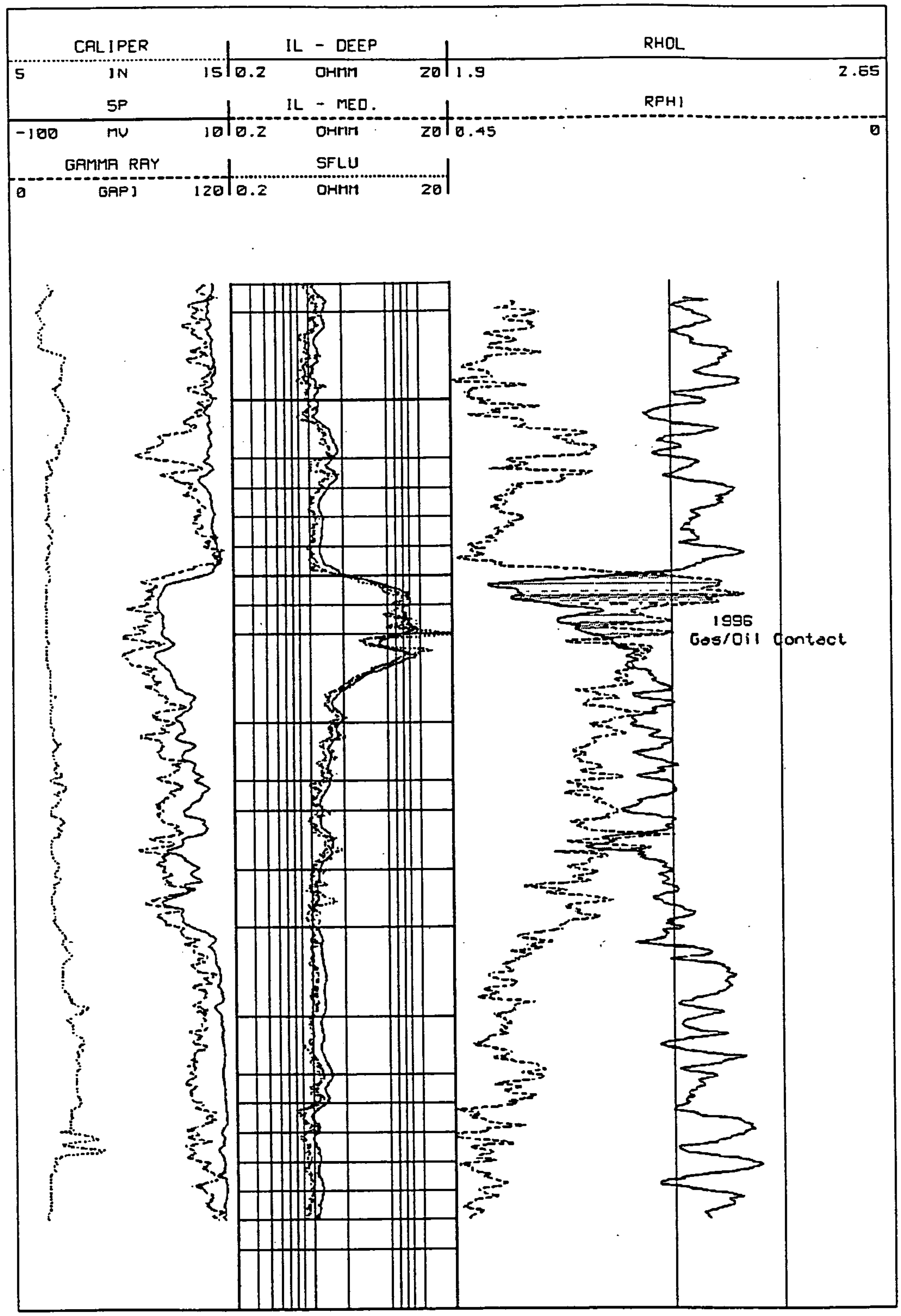
CALIPER
5 IN 15
SP
-100 MV 10
GAMMA RAY
0 GAPI 120
IL - DEEP
0.2 OHMM 20
IL - MED.
0.2 OHMM 20
SFLU
0.2 OHMM 20
RHOL
1.9 2.65
RPHI
0.45 0
1996
Gas/Oil Contact

Figure 12 - In Log Example 3, the porosity overlay of the density RHOL from LRHO and the cased-hole neutron porosity RPHI are used to target the oil production in the reservoir sand.

Analysis of the open-hole logs indicated that the original density log was questionable. In the reservoir sequence, the OH density porosity has readings in the 40 to 60 p.u. range, where nominal shale values in this area are in the 18 to 25 p.u. range. Many of the bad sections are in conjunction with bad hole events on the caliper, indicating that lack of pad contact may be the culprit. In the gas section of the reservoir sand, the hole was in gauge, but the OH density wanders past without correlation.

Modeling results[4] have demonstrated that this new method of density measurement has a deeper depth of investigation compared to the OH density. Another feature is that, for the centric geometry, hole rugosity is only a minor part of the borehole term and has little effect on the porosity measurement.

Further up the hole, the OH density seems to be correct over a water-sand sequence. In Figure 10 the LRHO curve is overlain with RHOB from open hole. The correlation of the two density measurements is plotted in Figure 11, and the average error (square root of the mean-squared error) is 0.052 g/cc in the section with good hole conditions. At the top and bottom of the interval, the hole condition deteriorates, and again the OH density goes to errantly low readings which are the outliers on Figure 11.

The fit error of 0.052 g/cc is not a great fit (3.2 p.u. error) but should be sufficient to normalize the PN density to this borehole environment. The cased-hole neutron density porosities were generated for the reservoir sequence (see Figure 12), and the analysis indicated that the top of the target sand is gas. The sand was completed in the oil section with production of 357 BOPD, 363 MCFD and 0 BWPD.

Log Example # 4 (Refer to Figure 13).

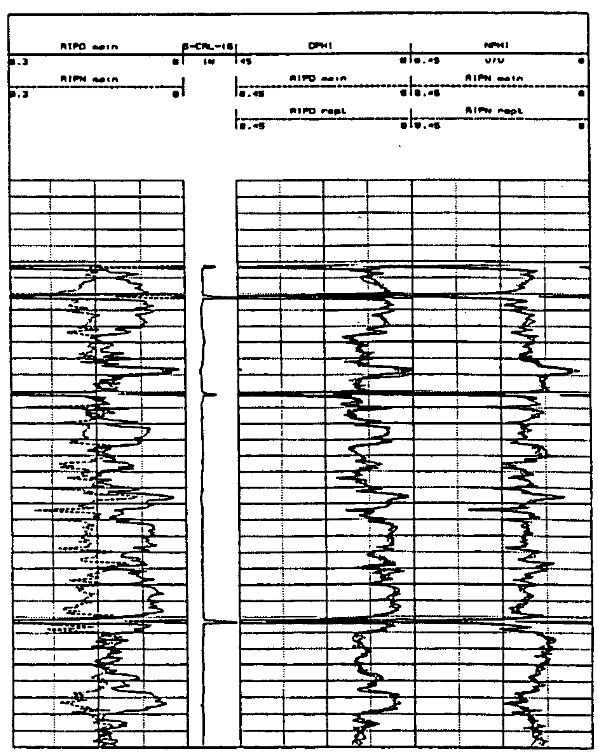

Figure 13 - Log Example 4 demonstrates the PND density response in the lower porosity range. The outputs from the BHC algorithm for a main pass and a repeat are overlain with the open hole data. In track one the cased-hole porosity overlay is shown on an expanded scale to show gas versus tight response.

This well is from the Texas Gulf Coast in the Wilcox sand. The PND-S system was used for analysis of the bottom 500 feet of the reservoir when open-hole logging tools could not get to bottom. We have included this example because it demonstrates two points: It shows system response at the low-porosity end (gas vs. tight); and, the correlation with open hole demonstrates how a BHC algorithm may ultimately be very accurate with good precision (repeatability).

In Figure 13, a section of the log is plotted with the cased-hole and open-hole porosities. The PND-S prototypical algorithm generates AIPD, the density porosity, and AIPN, the neutron porosity, that are overlain with the open-hole porosities. In track one the PND-S porosities are overlain to show the gas vs. tight response, and in tracks two and three the open-hole and cased-hole porosities are overlain to show correlation. The average error (the square root of the mean-squared error, compared to the open-hole measurements) of the cased-hole density and neutron porosities are 1.77 p.u and 1.93 p.u. respectively, over the 750 foot overlapping interval. The PND-S porosities from the repeat passes are also in tracks two and three to demonstrate the measurement's precision (average error of AIPD = 1.50 p.u., average error of AIPN = 1.17 p.u.).

Conclusions

The measurement of the formation density behind casing has long been the desire of engineers involved in cased-reservoir analyses. This powerful analysis tool has been developed for the 1.625 inch (and 1.6875 inch) Computalog PND-S pulsed neutron decay system. Specific characterization of the cased-hole density measurement can generate a density porosity that compares favorably with the open-hole, gamma-gamma density porosity. Characterization experiments on two sets of wells suggest that the development of a stand-alone quantitative algorithm may be possible.

Acknowledgments

The authors wish to thank Computalog and Chevron for allowing us to publish this data, and to the other oil companies that have supplied data and comments. Also a thank you and acknowledgment for the fine editing, graphics, data-processing done by Shawn Bailey.

Nomenclature

PN density=Density from pulsed neutron

OH density=Density from open-hole logging

NPHI = Open-hole compensated neutron porosity

DPHI = Open-hole gamma-gamma density porosity

RPHI = Cased-hole neutron porosity from PND-S ratio

LRHO = Gamma-ray diffusion length calculation

RHOL = Density from LRHO calculation

RHOB = Density from OH density

FPHI = Porosity from the far detector inelastic count rate

MeV = Mega electron volts

BOPD = Barrels of oil per day

BWPD = Barrels of water per day

MCFD = 1000 cubic feet units of gas per day

BHC = Borehole compensated

AIPD = Density porosity from BHC algorithm

AIPN = Neutron porosity from BHC algorithm

MWD = Measurement while drilling

SW-ARCHIE=Water Saturation from Open-Hole Resistivity

SW-PNC=Water Saturation from Sigma

References

1. Scheibal, J.R., Weiland, J.L., Worrel, J.M., Bayer, J.E.: "Differentiation of Hydrocarbon Type in Laminated Pliocene/Pleistocene Turbidite Sands Via Inelastic Pulsed Neutron Capture Data" paper SPE 24737 presented at the 67th Annual Technical Conference of SPE, Washington, DC, October 4 – 7, 1992.
2. Odom, R.C., Streeter, R.W., Hogan II, G.P., and Tittle, C.W.: "A New 1.625" Diameter Pulsed Neutron Capture and Inelastic/Capture Spectral Combination System Provides Answers in Complex Reservoirs," paper O presented at the 1994 SPWLA Annual Logging Symposium, Tulsa, OK, June 19 – 22.
3. Streeter, R.W., Hogan II, G.P., Rogers, C.B., Odom, R.C., Barrett, D.G.: "Cased Hole Exploration: Modern Pulsed Neutron Techniques for Locating By-Passed Hydrocarbons in Old Wells," Paper SPE 35162 presented at the 1996 Permian Basin Oil & Gas Recovery Conference, Midland, TX, March 27 – 29.
4. Wilson R.D.: "Bulk Density Logging With High-Energy Gammas Produced by Fast Neutron Reactions with Formation Oxygen Atoms," 1995 IEEE Nuclear Science Symposium, San Francisco, CA, October 25 – 28.
5. Tittman, J. and Wahl, J.S.: "The Physical Foundations of Formation Density Logging (Gamma-Gamma)," GEOPHYSICS (April 1965) XXX, No. 2.
6. Odom, R.C.: "Pulsed Neutron Decay Tool for Measuring Gamma Radiation Energy Spectra for Fast Neutron Inelastic Collisions and Thermal Neutron Capture Events," United States Patent Number 5,374,823 issued December 20, 1994.